

## Uncertainty Recognition and Quantification of Hydrologic Prediction

Shen CHIANG\*, Yasuto TACHIKAWA, Kaoru TAKARA

\*Graduate School of Engineering, Kyoto University

### Synopsis

We propose a methodology to identify prediction uncertainty through recognizing and quantifying the different uncertainty sources in a hydrologic model. Statistical second moment is used as a measure of uncertainty; also an index which originated from Nash coefficient of efficiency named Model Structure Indicating Index (MSII) is proposed to quantify model structure uncertainty. The results show that MSII can well reflect the goodness of model structure, while a larger value of MSII indicating a poorer structure of hydrologic model. The index can be used as a tool for implementing model quantitative comparison (selection).

**Keywords:** prediction uncertainty, Monte Carlo simulation, hydrological modeling

### 1. Introduction

Hydrological modeling is the discovery of general laws and principles that govern the natural phenomenon under observation. A hydrologic model is an integration of mathematical descriptions of conceptualized hydrologic processes, which serves for a specific purpose. Consequently, the spatial scale, temporal scale, structure, architecture, and applicability of a model are restricted a lot by the hypothesis of the hydrologic model in most of the cases. As a result, there are numerous hydrologic models developed for various aspects, and the development of new hydrologic models or improvement of previously developed models continues in Japan and elsewhere. With rapid advances in computing technology, remote sensing, GIS and DBMS, the role of hydrologic models is enhanced as a tool in planning, decision making and tends to incorporating with other process models such like economic, social, political, administrative, and judicial models. Thus, the watershed hydrologic models will become a component in a larger management strategy. Furthermore, these models will become more global, not only in the sense of spatial scale but also in the sense of hydrologic details (Singh, 2002). Therefore, a methodology to assess

the error, uncertainty and adequacy of adopting hydrologic models in specific purpose is needed. The present study provides a methodology for model comparison and selection through model uncertainty recognition and quantification.

For many years hydrologists have been interested in the effects of various uncertainties on the accuracy and reliability of the estimation of catchment hydrological variables such as peak flow and flood volume (Høybye and Rosbjerg, 1999). Among early contributions, some of them focus on the rainfall uncertainty and its influence to the runoff (e.g., Storm *et al.*, 1989); some of them focus on the sensitivity of model structure due to the input error (e.g., Singh and Woolhiser, 1976). Recent researches relating to hydrologic model uncertainty most refer to parameter uncertainty identification, the procedure of parameter calibration, and their impact to simulation result (e.g., Freer *et al.*, 1989; Kuczera and Parent, 1998). Among them, Generalized Likelihood Uncertainty Estimation (GLUE) Methodology (Beven and Binley, 1992) offers a path of identifying parameter uncertainty. Nevertheless, parameter equifinality became the conclusion of GLUE; uncertainty related to input data and other factors are excluded. Even it is said that they could also be included in GLUE but this has not normally been done (Beven, 2001).

The performance of hydrologic models is profoundly affected by the sources of uncertainty, briefly they are:

- (a) Observed data,
- (b) Data for model calibration,
- (c) Parameter space, and
- (d) Model structure.

Among those, data uncertainty occupies the most and contaminates other sources of uncertainty. Underestimating or misunderstanding of these uncertainty sources and the interrelation among them may cause tremendous misleading on interpreting the result of hydrologic models. However, recognizing and quantifying these different sources of uncertainty in hydrologic models has received little attention in the research literature.

In this study, a methodology is proposed to recognize and quantify the different uncertainty sources. Firstly, Monte Carlo simulation method is applied to add bias item in model input data series (rainfall), then rainfall realizations, parameter space, and model outcomes (outflow discharge) under different bias level are acquired. Secondly, by examining the counter relationship between model simulation outcomes, calibration outcomes and observed watershed response series (discharge), an uncertainty structure is recognized. Finally, parameter uncertainty, calibration uncertainty, and model structure uncertainty caused by input data uncertainty are recognized, separated, and quantified through the methodology.

Statistical second moment is used as a measure of uncertainty, also an index which originated from Nash coefficient named Model Structure Indicating Index (MSII) is proposed to quantify model structure uncertainty which can be used as a tool for implementing model quantitative comparison (selection). For the demonstration of the proposed method, several hydrologic models are applied to perform model comparison. They are: Storage Function Method (SFM, Kimura, 1961), Topmodel (Kirkby and Beven, 1986) and KW-GIUH (Lee and Yen, 1996). Through fixing the value of one parameter of SFM, a poorer structure model is formed as an extreme contradistinction.

The results show that a larger value of MSII indicating a poorer structure of hydrologic model in a dynamic manner, that is, incorporating the MSII to the input uncertainty.

## 2. Uncertainty recognition in hydrological modeling

In this study, prediction uncertainty which came from the four kinds of sources mentioned previously is classified into four categories: system uncertainty,

entire uncertainty, inherent uncertainty, and structure uncertainty. The definition and the procedure to recognize them are described below.

### 2.1 System uncertainty

Even it is well known that a hydrologic model is an approximation of the real phenomena based on the hydrologic cycle, still it is needed to stress that there always existing discrepancy between model outcome and observed data, no matter how precise the model is and how perfect the model calibrated. That is the model predicting limitation underneath the hypothesis and architecture of the model, which is defined as the system uncertainty in this study.

The system uncertainty can be recognized by evaluating the discrepancy between observed watershed response series and the model outcome during the process of model parameter calibration. This can be clarified by the statement written below:

$$\tilde{y} = f(\tilde{x}, \theta) \quad (1)$$

where  $\tilde{y}$  and  $\tilde{x}$  denote outcome and input series of a hydrologic model  $f(\cdot)$  respectively, and  $\theta$  denotes a parameter set. Denoting  $X$  and  $Y$  are observed watershed input and response series data accordingly and assuming  $\tilde{x} = X$ , then  $\theta$  can be determined by adjusting or tuning the value of parameters to make the difference between model outcome  $\tilde{y}$  and observed watershed response data  $Y$  in an acceptable range according to some objective function. The procedure of adjusting the value of parameter set is well known as "model calibration". In this study, least sum of square error (LSE) method is selected as the objective function:

$$S_{LS}(\theta_m) = \sum_{n=1}^N (Y_n - f(X_n, \theta_m))^2 \quad (2)$$

where  $n$  denotes time step of the simulation time series;  $m$  denotes the parameter set to be examined.

The discrepancy between observed watershed response and model outcome during the process of calibration is supposed to be the minimum value by comparison to the possible coming events. This has often been observed that the goodness-of-fit between observed data and estimated data during calibration is better than what in validation, not to mention in implementation. Under this fact, we can say that the uncertainty occurring here denotes the predicting limitation of the model. Since this is the best that a model can achieve.

### 2.2 Entire uncertainty

The discrepancy of the model outcome to the observed data can be shown as below:

$$Y = f(X, \theta) + \varepsilon \quad (3)$$

where  $\varepsilon$  denotes system uncertainty mentioned above, that is, the predicting limitation of the model under perfect calibration. In agreement with this definition, it is clear that the uncertainty came from the process of calibration. But the real uncertainty source is supposed to be the data which is used for calibration.

After calibrating the model parameter, the calibrated parameter space will reflect its uncertainty through the model structure and propagates to the model outcome. This uncertainty can be recognized by examining the discrepancy between observed watershed response data and model outcome by using input data and parameter sets. Also this is the way of most of the researches dealing with parameter sensitivity. This uncertainty is defined as the entire uncertainty in this study, since actually this is the utmost uncertainty a model could have under existing input uncertainty.

### 2.3 Inherent uncertainty

Another categorized uncertainty what we called "inherent uncertainty" is very difficult to be recognized since it is always contaminated by the uncertainty of model structure and input data. Inherent uncertainty is different to what so called parameter uncertainty since the propagation effect of

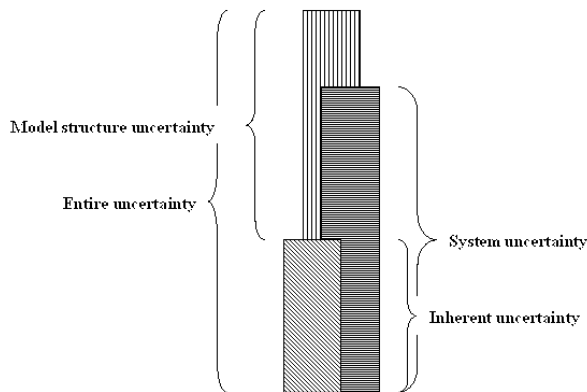


Fig. 1 Schematic diagram of the uncertainty structure



Fig. 2 Schematic diagram of the uncertainty acquisition process

model structure is excluded here intentionally. Inherent uncertainty represents the sensitivity of parameter space which determined according to the input uncertainty and reflects to model outcomes. This can be examined by the discrepancy among model outcomes derived from different best fit parameter sets. Watershed response data is not used here, which indicates the model structure uncertainty is eliminated as much as possible.

### 2.4 Structure uncertainty

The distance between entire uncertainty and inherently uncertainty is structure uncertainty. Since the parameter set used for extracting both of the uncertainty is the same. The different is the data used for comparison: observed data and outcome during calibration. The propagation effect plays an

important role here, which is why the difference between entire uncertainty and inherent uncertainty is called structure uncertainty in this study.

The schematic diagram of uncertainty structure proposed here is depicted in Fig.1, which reveals a static view of model uncertainty structure, that is, the input uncertainty (data uncertainty) is neglected or fixed to a certain magnitude. In order to know the behavior of model structure uncertainty under different input uncertainty level, a dynamic view of model uncertainty structure is introduced by increasing the input uncertainty during the processes of uncertainty recognition. The behavior of model structure uncertainty under different input uncertainty can be examined by observing the discrepancy among different model outcomes accordingly. Fig.2 shows the schematic diagram of the uncertainty acquisition process. By increasing the magnitude of the bias item (input uncertainty) which located in the center of the diagram, the subsequent change of different categorized uncertainty can be observed and evaluated. It is expected that within certain level of input uncertainty, model with a better structure still capable to reflect the true catchment hydrologic behavior in certain level.

### 3. Uncertainty quantification

Several indexes are selected to perform uncertainty quantification in this study; the basic form of the index is statistical second moment and Nash coefficient.

The categorized prediction uncertainties defined in previous section are mathematically described as below:

### 3.1 Index for quantifying system uncertainty

$$Nash_s = 1 - \frac{\sqrt{\sum (Q_o - Q_b)^2}}{\sqrt{\sum (Q_o - \bar{Q}_o)^2}} \quad (4)$$

where  $Q_o$  and  $Q_b$  indicate the observed watershed response series and model outcome by using the best fit parameter set,  $n$  is the time step of the time series.  $SD_s$  quantifies the error variance, the residuals, between observed watershed response and the best fitted simulated outcomes; while  $Nash_s$  elucidates the performance of the best fitted simulated outcomes.  $SD$  always larger than 0, while the range of  $Nash$  coefficient is:  $-\infty < Nash \leq 1$ .

### 3.2 Index for quantifying entire uncertainty

$$Nash_e = 1 - \frac{\sqrt{\sum (Q_o - Q_e)^2}}{\sqrt{\sum (Q_o - \bar{Q}_o)^2}} \quad (5)$$

where  $Q_e$  is the model outcomes acquired by using a parameter set within the whole parameter space and entire rainfall realizations. Consequently,  $SD_e$  explains the total prediction error.

### 3.3 Index for quantifying inherent uncertainty

$$Nash_i = 1 - \frac{\sqrt{\sum (Q_b - Q_e)^2}}{\sqrt{\sum (Q_b - \bar{Q}_b)^2}} \quad (6)$$

$SD_i$  and  $Nash_i$  explain the inherent uncertainty because  $Q_e$  is calculated with a possible parameter set identified by other model outcomes, thus, the discrepancy between  $Q_b$  and  $Q_e$  indicates the error inevitable in a model formulation.

### 3.4 Index for structure uncertainty

In order to implement dynamic view of the relationship among system uncertainty, structure uncertainty and parameter uncertainty caused by input data uncertainty, the Nash coefficient is used to formulate a Model Structure Indicating Index (MSII) and is defined as:

$$MSII = \frac{Nash_i - Nash_e}{Nash_s} \quad (7)$$

The difference between entire and inherent uncertainty denotes the structure uncertainty. This

is used as the numerator in the equation, while system uncertainty is used as a denominator to form a criterion to evaluate model structure. The index expresses the total variance unexplained by the standard deviation in a dimensionless form. The range of MSII is:  $0 \leq MSII < \infty$ .

## 4. Algorithm for uncertainty recognition & quantification

Instead of sampling the parameter space directly like what GLUE did, the study here generates the parameter set space by introducing noise item into input data with specified probability distribution. Here Normal distribution with mean equals to zero and standard deviation from 1.0 to 9.0 (mm/hr) is used to acquire model parameter space and outcomes under different input uncertainty. For each iteration, 10000 model outcomes for each specified input uncertainty were derived from the combination of rainfall series and parameter set generate output series through the model. The system uncertainty and the prediction ability were identified and recognized by corresponding parameter set. Detail algorithm for uncertainty recognition and quantification is listed in Fig.3.

## 5. Model description and process of observed data

To demonstrate uncertainty identification, Storage Function Model (SFM) proposed by Kimura (1975), Topmodel (Kirkby and Beven) and KW-GIUH are applied at the Yasu River basin (355km<sup>2</sup>) in this study. Below are the brief description of the models.

### 5.1 Storage Function Model:

The form of SFM is as:

$$\frac{dS}{dt} = r_e(t - T_l) - q, \quad S = kq^p \quad (8)$$

$$r_e = \begin{cases} f \times r, & \text{if } \sum r \leq R_{SA} \\ r, & \text{if } \sum r > R_{SA} \end{cases}$$

where  $S$  = water storage height;  $r$  = rainfall intensity;  $q$  = runoff height;  $t$  = time step; and  $T_l$  = the lag-time.

This model is often used for the flood runoff calculation in a basin with an area of less than five hundred square kilometers in Japan (Takara and

For input uncertainty  $\sigma_x = 1.0, 2.0, \dots, 8.0, 9.0$  (unit: mm/hr)

1. Use Monte Carlo simulation to sample 100 rainfall realizations according to a real recorded event by adding noise item to it.
2. Use LSE to determine 100 parameter sets

regarding to its corresponding rainfall realization.

$$S_{LS}(\theta_j) = \min\left(\sum_{n=1}^N (Y_n - f_n(\bar{x} + \xi_j, \theta_j))^2\right), j = 1, \dots, 100$$

3. System uncertainty  $\varepsilon_s$  is acquired by examining the discrepancy between 100 best fit model outcomes during calibration and observed watershed response. Mean value of  $SD_s$  and  $Nash_s$  for 100 cases are used for uncertainty quantification.

$$Y = f(\bar{x} + \xi_j, \theta_j) + \varepsilon_s, j = 1, \dots, 100$$

4. Entire uncertainty  $\varepsilon_e$  is acquired by examining the discrepancy between observed watershed response and 10000 model outcomes. Mean value of  $SD_e$  and  $Nash_e$  for 10000 cases are used for uncertainty quantification.

$$Y = f(\bar{x} + \xi_j, \theta_j) + \varepsilon_e;$$

$$j = 1, \dots, 100; k = 1, \dots, 100$$

5. Inherent uncertainty  $\varepsilon_i$  is acquired by examining the discrepancy between 100 best fit model outcome during calibration and the rest 9900 model outcome. Mean value of  $SD_i$  and  $Nash_i$  for 10000 cases are used for uncertainty quantification.

$$y_l = f(\bar{x} + \xi_l, \theta_k) + \varepsilon_i, l \neq k;$$

$$l = 1, \dots, 100; k = 1, \dots, 100$$

$$y_l = f_l(\bar{x} + \xi_l, \theta_l), l = 1, \dots, 100$$

6. Apply Eq. (10) to acquire MSII of the Model.  
End

where  $\xi \sim N(0, \sigma_x^2)$ ,  $n$  denotes time step of the simulation time series,  $\bar{x}$  denotes the observed input data series.

Fig. 3 Algorithm for uncertainty recognition and quantification

Takasao, 1985). Parameter  $p$  is a constant, commonly the value is 0.6,  $f$  is the ratio of contribution area of the watershed which generates outflow,  $R_{SA}$  is accumulating saturated rainfall. Parameter  $k$  is solved by the equation proposed by Nagai *et al.* (1982).

A fully functional SFM with parameter  $T_b$ ,  $f$ , and  $R_{SA}$  is used. For contradistinction, a poorer-structured model with comparison to the original SFM by fixing the value of  $R_{SA}$  to 0.0 is manipulated in this study.

## 5.2 Topmodel

Topmodel is a set of programs for rainfall-runoff modeling in single or multiple subcatchment in a semi-distributed way and using gridded elevation data for the catchment area. It is considered a physically based model as its parameters can be, theoretically measured in situ (Beven and Kirkby,

1979, Beven *et al.*, 1984). In this study, TOPMODEL 95.02, written in FORTRAN 77 is used.

Topmodel uses the distribution of the topographic index of hydrological similarity:

$$\lambda_i = \ln\left(\frac{a_i}{\tan \beta_i}\right) \quad (9)$$

where  $a_i$  (unit: m) is the specific contribution area, which denotes the area draining through a grid cell per unit length of contour.  $\tan \beta_i$  denotes the local surface slope. Flow is separated into surface runoff generated by rainfall on saturated contributing area and subsurface downhill flow. There are four basic assumptions to relate local downslope flow from a point to discharge at the catchment outlet (Campling *et al.*, 2002):

A1. The dynamics of the saturated zone are approximated by successive steady state representation.

A2. The recharge rate  $r$  (m/h) entering the water table is spatially homogeneous.

A3. The effective hydraulic gradient of the saturated zone is approximated by the local surface topographic gradient  $\tan \beta_i$ .

A4. The distribution of downslope transmissivity  $T_o$  ( $m^2/h$ ) with depth is a function of storage deficit.

From A1 and A2, the recharge rate of the flux drains into the water table has the form like:

$$q_i = ra_i = T_o e^{-S_i/m} \tan \beta_i \quad (10)$$

where  $q_i$  is the flux drains into the water table for topographic index class  $i$ .  $r$  denotes recharge rate the water drains to the water table, and  $S_i$  is a local storage deficit, and  $m$  is a model parameter controlling the rate of decline of transmissivity with increasing storage deficit.

By arranging Eq.(10), the local storage deficit  $S_i$  can be calculated:

$$S_i = -m \ln\left(\frac{ra_i}{T_o \tan \beta_i}\right) \quad (11)$$

The mean catchment storage deficit  $\bar{S}$  can be obtained by integrating Eq.(11) over the entire catchment area  $A$ :

$$\bar{S} = \frac{1}{A} \sum_i A_i \left( -m \ln \frac{ra_i}{T_o \tan \beta_i} \right) \quad (12)$$

where  $A_i$  is the fractional area of the topographic index class  $i$ . Then storage deficit of each topographic index  $i$  can be expressed like below:

$$S_i = \bar{S} + m \left( \bar{\lambda} - \ln \frac{a_i}{\tan \beta_i} \right) \quad (13)$$

where  $\bar{\lambda}$  is the areal average of the topographic index  $\ln \frac{a}{\tan \beta}$  of whole catchment.

$$\bar{\lambda} = \frac{1}{A} \int_0^A \ln \left( \frac{a_i}{\tan \beta_i} \right) A_i dA \quad (14)$$

The vertical drainage  $q_v$  from unsaturated zone storage at any point I is calculated by Eq.(15) below:

$$q_v = \frac{S_{uz}}{S_i t_d} \quad (15)$$

where  $S_{uz}$  is the storage in the unsaturated zone, and  $t_d$  is a time delay constant. The total vertical drainage then can be calculated by summing up the flux along catchment area.

$$Q_v = \sum q_v A_i \quad (16)$$

Output discharge from saturated zone can be calculated using a subsurface storage deficit-discharge function of the form:

$$Q_b = Q_0 e^{-\bar{S}/m} \quad (17)$$

where  $Q_0 = A e^{-\bar{\lambda}}$  is the discharge when  $\bar{S}$  is zero.

At each topographic index class  $i$ , unsaturated and saturated zone fluxes are simulated. Initial base flow  $Q_0$  and the initial root zone storage deficit  $S_{r0}$  are specified at the start of simulation. For the following time step, the average storage deficit is calculated according to Eq. (18). By which the catchment average storage deficit  $\bar{S}$  is updated by subtracting the unsaturated zone recharge and adding the baseflow from the previous time step:

$$\bar{S}_t = \bar{S}_{t-1} + [Q_{bt-1} - Q_{vt-1}] \quad (18)$$

Topographic index derivation was obtained by using DEM algorithm. Infiltration excess mechanism is not included in the study. Subcatchment discharge is routed to the catchment outlet by using time-area curve which generated from dem-based algorithm with constant velocity all over the catchment area.

### 5.3 KW-GIUH

If one unit rainfall excess fall on the watershed instantaneously at time  $t=0$ , by assuming that the raindrops are independent and isolated from each other and ignoring the raindrops fall on the river, then the distribution of the number of raindrop appears at the outlet to time is the instantaneous unit hydrograph of the watershed.

For a watershed of  $\Omega$  order which categorized under the Horton-Strahler ordering scheme, the path of a raindrop drains to the outlet of the watershed will follow the sequence from a lower order overland flow phase to a stream flow phase then a higher order stream finally outlet of the watershed. If  $w$  denotes a specified path  $x_{oi} \rightarrow x_j \rightarrow \dots \rightarrow x_\Omega$ , the probability of a drop of rainfall excess adopting this path can be expressed as

$$P(w) = P_{OA_i} \cdot P_{x_{oi}x_i} \cdots P_{x_i x_j} \cdots P_{x_k x_\Omega} \quad (19)$$

where  $P_{OA_i}$  is the ratio of the  $i$ th-order overland flow area to the total watershed area.  $P_{x_{oi}x_i}$  is the probability that rainwater drains from  $i$ th-order overland flow to  $i$ th-order stream, the value supposed to be 1 according to the assumption mentioned above;  $P_{x_i x_j}$  is the transitional probability of a raindrop from an  $i$ th-order stream to a  $j$ th-order stream, which is equal to the ratio of the number of  $i$ th-order stream drains to  $j$ th-order stream divided by the number of  $i$ th-order stream.

Since the raindrops are assumed to behave independently and isolated to each other, the storage inside the watershed at time  $t$  equals to the number of raindrops that the travel time  $T$  to the outlet larger than  $t$ .

Let  $f_{x_j}(t)$  represents the distribution of travel time that a raindrop moving in  $x_j$  phase, and the average of  $f_{x_j}(t)$  is  $T_{x_j}$ , then the storage can be shown as (Feller, 1968):

$$P(T \leq t) = \sum_{w \in W} \left[ \int_0^t f_{x_w}(t') * f_{x_i}(t') * f_{x_j}(t') * \dots * f_{x_\Omega}(t') dt' \right] \cdot P(w) \quad (20)$$

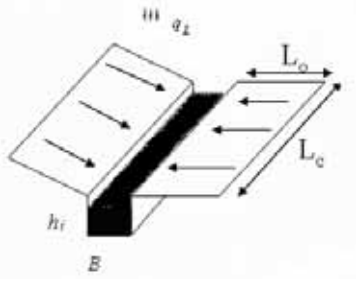


Fig. 4 V-shape subbasin

among it, \* denotes convolution integral. Since the raindrops are assumed to behave independently and isolated to each other, the storage inside the watershed at time  $t$  equals to the number of raindrops that the travel time  $T$  to the outlet larger than  $t$ . For one unit of rainfall excess,  $I(t) = 1.0$  when  $t=0$ ; and  $I(t) = 0$  when  $t \neq 0$ , then the outflow hydrograph  $u(t)$  at the outlet of the watershed is the instantaneous unit hydrograph of the watershed. From Eq. (20) we can get (Rodriguez-Iturbe and Valdes, 1979; Gupta et al., 1980).

$$u(t) = \sum_{w \in W} [f_{x_{oi}}(t) * f_{x_i}(t) * f_{x_j}(t) * \dots * f_{x_{\Omega}}(t) dt] \cdot P(w) \quad (21)$$

The following procedure is the determination of the distribution function for the travel time.

KW-GIUH (Lee and Yen, 1997) is a refinement of the GIUH method by using kinematic wave approximation to calculate the travel time of overland flow inside the catchment.

In KW-GIUH, an  $i$ th-order subbasins of the watershed conceptually simplified as consisting of two identical rectangular overland-flow planes. Each plane contributes a lateral discharge into a channel of constant cross section and slope as shown as in Fig.4.

Assuming rainfall excess with intensity  $q_L$  fall on the plane homogeneously, the continuity equation and simplified momentum equation can be expressed as:

$$\frac{\partial h_{oi}}{\partial t} + \frac{\partial q_{oi}}{\partial x} = q_L \quad (22)$$

$$q_{oi} = \alpha_o h_{oi}^m \quad (23)$$

where  $x$  is the distance along flow direction;  $h_{oi}$  is the  $i$ th-order overland flow depth;  $q_{oi}$  is  $i$ th-order overland flow discharge per unit width;  $m$  is constant,  $\alpha_o$  is the parameter which reflects the hydraulic characteristics of the overland flow, and  $q_L$  is lateral

inflow rate joining the main stream flow  $q_{oi}$ .  $\alpha_o$  can be expressed as:

$$\alpha_o = \frac{\sqrt{\bar{S}_{oi}}}{n_o} \quad (24)$$

where  $\bar{S}_{oi}$  is the mean slope of the  $i$ th-order overland flow, and  $n_o$  is an effective roughness coefficient for the overland flow plane, which is a parameter of the model need to be calibrated. The flow rate at the end of a plane increases with time until it reaches equilibrium. The longest time for a raindrop to travel through the  $i$ th-order overland plane  $T_{xoi}$ , is the time for the flow to reach equilibrium in the plane. Thus, the discharge for the  $i$ th-order overland subbasin at any time  $t < T_{xoi}$  is:

$$q_{oi} = q_L \bar{L}_{oi} = \frac{\sqrt{\bar{S}_{oi}}}{n_o} h_{oi}^m \quad (25)$$

then travel time  $T_{xoi}$  can be calculated by(Wooding, 1997):

$$T_{xoi} = \frac{h_{oi}}{q_L} = \left( \frac{n_o \bar{L}_{oi}}{\bar{S}_{oi}^{1/2} q_L} \right)^{1/m} \quad (26)$$

Since the overland flow will concentrate to the channel on the center of the V-shape plain eventually, for a channel with channel width  $B_i$ , the lateral discharge per unit width when it is equilibrium status is  $2q_L \bar{L}_{oi} / B_i$ , then the travel time of  $i$ th-order channel flow can be expressed as(Lee and Yen, 1997):

$$T_{xi} = \frac{B_i}{2q_L \bar{L}_{oi}} \left[ \left( h_{co_i}^m + \frac{2q_L n_c \bar{L}_{oi} \bar{L}_{ci}}{\bar{S}_{ci}^{1/2} B_i} \right)^{\frac{1}{m}} - h_{co_i} \right] \quad (27)$$

where  $\bar{S}_{ci}$  is the mean slope of the  $i$ th-order channel flow, and  $n_c$  is an effective roughness coefficient for the channel flow, which is a parameter need to be calibrated,  $h_{co_i}$  is the water depth that drains from upstream channel to the  $i$ th-order channel. For an  $\Omega$  order watershed, when  $i=1$ ,  $h_{co_i}=0$ ; when  $1 < i < \Omega$ ,  $h_{co_i}$  can be expressed as(Lee and Yen, 1997):

$$h_{co_i} = \left[ \frac{q_L n_c (N_i \bar{A}_i - AP_{O_{A_i}})}{N_i B_i \bar{S}_{c_i}^{1/2}} \right]^{\frac{1}{m}} \quad (28)$$

among it,  $N_i$  is the number of the  $i$ th-order channels;  $\bar{A}_i$  denotes the average area of  $i$ th-order subbasin, the area is not  $i$ th-order subbasin but also its upstream area is included.  $A$  = total area of the watershed;  $P_{O_{A_i}}$  is the ratio of the  $i$ th-order overland flow area to the total watershed area..

The mean length of the  $i$ th-order V-shape overland flow planes is:

$$L_{oi} = \frac{AP_{O_{A_i}}}{2N_i \bar{L}_{c_i}} \quad (29)$$

$\bar{L}_{c_i}$  is the mean channel length of the  $i$ th-order subbasins. The channel width is derived by linear decreasing from the watershed outlet(Lee and Yen, 1997):

$$B_i = \frac{B_\Omega \sum_{l=1}^i \bar{L}_{c_l}}{\sum_{l=1}^{\Omega} \bar{L}_{c_l}} \quad (30)$$

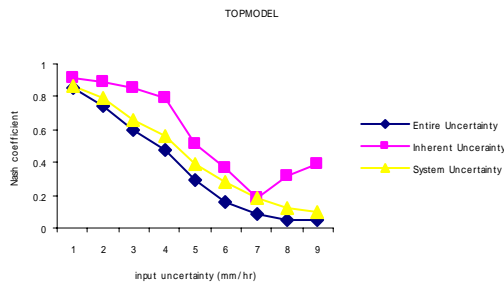


Fig. 5 Uncertainty quantification result of TOPMODEL

$B_\Omega$  is the channel width on the outlet of the watershed, which can be acquired by field survey. The rest of all the geomorphic factors can be acquired manually from topographic map or derived automatically through raster elevation data and DEMs by some algorithms.

Rainfall data was collected from four rainfall gauging stations inside the Yasu River basin (355km<sup>2</sup>); they are Yasu, Minakuchi, Kouka and Oogawara. The average precipitation was obtained by using Thiessen polygon method.

## 6. Results

Fig.5 through Fig.8 are the plot of TOPMODEL, SFM, parameter-constrained SFM and KW-GIUH. It can be seen that the entire uncertainty becoming larger while input uncertainty increasing. Also the magnitude of standard deviation of the categorized behaves the same. It is always expected that entire uncertainty increases while input uncertainty increasing; where the discrepancy between entire and inherent uncertainty is in the same tendency. System uncertainty is supposed located in the middle between entire and inherent uncertainty. The range between entire and inherent uncertainty indicates the goodness of a model structure; that is, the ability of a model simulates the behavior of the watershed through observed data. The broader the distance is the worse structure the model has.

The distance between entire uncertainty and system uncertainty indicates the divergence between calibration outcome and simulation outcome. Fig.9

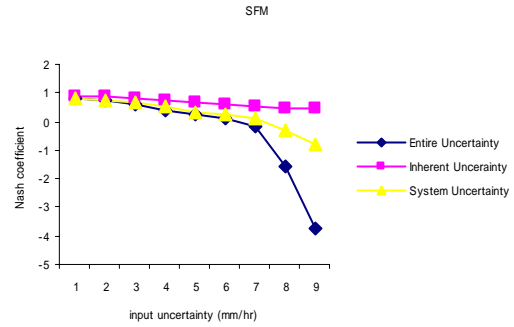


Fig. 6 Uncertainty quantification result of SFM

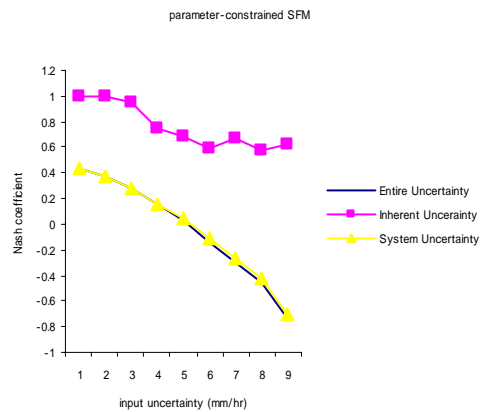


Fig. 7 Uncertainty quantification result of parameter-constrained SFM

shows the MSII of each model. Except parameter-constrained SFM, there is no apparent distinction between the four candidate models within



small input uncertainty. However, along with the increasing of the input uncertainty, KW-GIUH is structurally more stable than the TOPMODEL and SFM in this study.

## 7. Conclusions

For specific catchment, a methodology for uncertainty recognition and quantification is proposed which can be used as a tool for hydrologic models quantitative

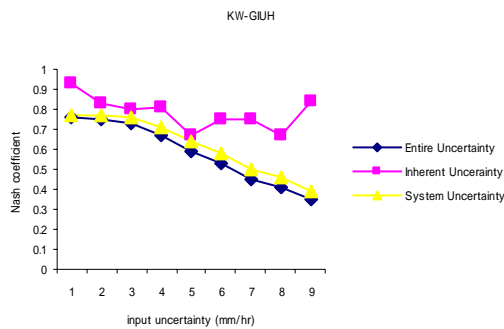


Fig. 8 Uncertainty quantification result of KW-GIUH

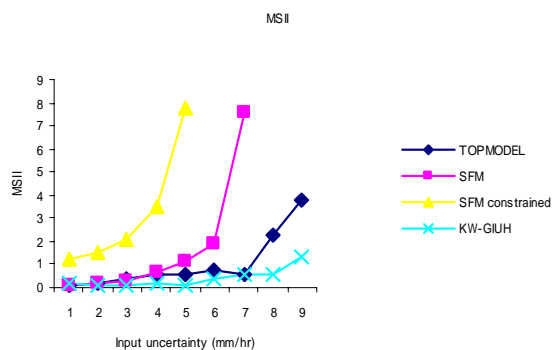


Fig. 9 MSII of TOPMODEL, SFM, parameter-constrained SFM and KW-GIUH

comparison or evaluation. Instead of sampling the parameter space directly like what GLUE did, the study here generates the parameter set space by introducing noise item into input data with specified probability distribution. This reflects the truth that parameter uncertainty came from uncertainty of data to hand and the way the model structure responses it. The results show that within increasing input uncertainty, the distance between entire and inherent uncertainty is also increased. A smaller magnitude of the ratio of inherent uncertainty to entire uncertainty indicates the system uncertainty (i.e. the prediction limitation) is larger, which means lacking of the ability to simulate the true watershed behavior. MSII is proposed to evaluate the goodness of model

structure. While a good model structure is defined as: Within certain level of input uncertainty, the model still capable to reflect the true catchment behavior. The results show that a larger value of MSII indicates a poorer structure of hydrologic model, within increasing input uncertainty the tendency becomes more apparently. The goodness of the process of model calibration is also included in the index explicitly. The index can be used as a tool for implementing model quantitative comparison (selection).

## Acknowledgments

A part of this study was supported by Grant-in-Aid for Scientific Research (A)(1) 16206050 (PI: Prof. K. Takeuchi, Yamanashi Univ.) and CREST program of JST (PI: Prof. K. Takara, Kyoto Univ.).

## References

- Beven, K. (2001): How far can we go in distributed hydrological modeling? *Hydrology and Earth System Science*, Vol. 5(1), pp. 1-12.
- Beven, K. J. and Binley, A. M. (1992): The future of distributed models: Model calibration and uncertainty prediction, *Hydrol. Proces.*, Vol. 6, pp. 279-298.
- Campling, P., Gobin, A., Beven, K. and Feyen, J. (2002): Rainfall-runoff modeling of a humid tropical catchment: the TOPMODEL approach, *Hydrological Process*, Vol. 16, pp231-253.
- Freer, J., Beven, K. and Ambrose, B. (1996): Bayesian estimation of uncertainty in runoff prediction and the value of data: An application of the GLUE approach, *Water Resources Research*, Vol. 32(7), pp. 2161-2173.
- Gupta, V. K., Waymire, E., and Wang, C. T. (1980): A representation of an instantaneous unit hydrograph from geomorphology, *Water Resour. Res.*, Vol. 16(5), pp.855-862.
- Høybye, J. and Rosbjerg, D. (1999): Effect of input and parameter uncertainties in rainfall-runoff simulation, *Journal of Hydrologic Engineering*, Vol. 4(3), pp.214-224.
- Kimura, T. (1975): *Storage Function Method*. Kawanabe Books Co., Ltd., Tokyo (in Japanese).
- Kuczera, G. and Parent, E. (1998): Monte Carlo assessment of parameter uncertainty in conceptual catchment models: the Metropolis algorithm, *Journal of Hydrology*, Vol. 211, pp. 69-85.
- Lee, K. T. and Ben, C. Y. (1997): Geomorphology and kinematic-wave-based hydrograph derivation, *Journal of Hydraulic Engineering*, Vol. 123(1), pp73-80.
- Nagai, A., Kadoya M., Sugiyama H. and Suzuki K. (1982): Synthesizing storage function model for flood runoff analysis. *Disaster Prevention*

- Research Institute Annuals, No. 25 B-2, pp. 207-220.
- Rodriguez-Iturbe, I. and Valdes, J. B. (1979): The geomorphologic structure of hydrologic response, *Water Resour. Res.*, Vol. 15(6), pp. 1409-1420.
- Sherman, L. K. (1932): Streamflow from rainfall by the unit-graph method, *Eng. New-Rec.*, 108, pp.501-505.
- Singh, V. P. and Woolhiser, D. A. (1976): Sensitivity of linear and nonlinear surface runoff models to input errors, *Journal of Hydrology*, Vol. 29, pp. 243-249.
- Singh, V. P. and Woolhiser, D. A. (2002): Mathematical modeling of watershed hydrology: *Journal of Hydrologic Engineering*, Vol. 7, pp. 270-292.
- Storm, B., Høgh Jensen, K. and Refsgaard, J. C. (1989): Estimation of catchment rainfall uncertainty and its influence on runoff prediction, *Nordic Hydro.*, Vol. 19, pp. 77-88.
- Takara, K. and Takasao, T. (1985): A new attempt to evaluate rainfall-runoff models from the viewpoint of stochastic transformation, *Journal of Hydroscience and Hydraulic Engineering*, Vol. 3(2), pp. 61-72.

## 水文モデル予測の不確かさの認出と定量化

江 申\*, 立川 康人, 宝 馨

\*京都大学大学院工学研究科土木工学専攻

### 要旨

本研究では、水文予測の不確かさを生み出すもとなる異なる要因を認識し定量化することにより、水文予測の不確かさを同定する手法を提案する。予測の不確かさを計量する手法として統計的な二次モーメントを利用する。またモデル構造の不確かさを定量化する指標として、Nash 指標を基にしたモデル評価指標 MSII (Model Structure Indicating Index) を提案する。MSII の値は、モデル構造が不適当なモデルほど大きな値を示す。この指標は水文モデルを予測の不確かさの観点から定量的に評価するために有効に利用することができる。

キーワード: 予測の不確かさ, モンテカルロシミュレーション, 水文モデリング, PUB